Available online at www.sciencedirect.com
ScienceDirect
Journal of the European Ceramic Society 27 (2007) 4391–4394
www.elsevier.com/locate/jeurceramsoc

# Synthesis and structural characterization of In-doped $ZnFe_2O_4$ nanoparticles

M. Maletin [a], Evagelia G. Moshopoulou [b,*], A.G. Kontos [c,d], E. Devlin [b], A. Delimitis [e], V.T. Zaspalis [e], L. Nalbandian [e], V.V. Srdic [a]

[a] *Department of Materials Engineering, Faculty of Technology, University of Novi Sad, Bul. Cara Lazara 1, 21000 Novi Sad, Serbia*
[b] *Institute of Materials Science, NCSR "Demokritos", 15310 Agia Paraskevi, Greece*
[c] *Physics Department, National Technical University of Athens, 15780 Athens, Greece*
[d] *Institute of Physical Chemistry, NCSR "Demokritos", 15310 Agia Paraskevi, Greece*
[e] *Chemical Process Engineering Research Institute (CPERI), CERTH, P.O. Box 361, 57001 Thessaloniki, Greece*

Available online 8 April 2007

**Abstract**

In-doped $ZnFe_2O_4$ nanoparticles were prepared by a co-precipitation method. The nanoparticles were charactarized by conventional powder X-ray diffraction, energy dispersive X-ray spectrometry, transmission electron microscopy, Raman and Mössbauer spectroscopy. It was found that $Zn_{1-x}In_xFe_2O_4$ nanoparticles of size ≈4 nm can be formed for $0 \leq x \leq 0.6$. However, only for $0 \leq x \leq 0.15$, was it possible to obtain single phase samples. These new $Zn_{1-x}In_xFe_2O_4$ ($0 \leq x \leq 0.6$) nanoparticles exhibit behavior distinct from their bulk counterparts and present an evolution of the structural and physical properties as a function of $x$. Detailed results, as well as the interest of these materials both for applied and basic science perspectives will be presented.


*Keywords:* Co-precipitation; Ferrites; Magnetic properties

## 1. Introduction

At present, one of the most interesting and challenging issues of the science of magnetic nanoparticles is the introduction of new electronic, optical or photochemical properties and the optimization of their magnetic properties. Such novel nanoparticles are very interesting both from the fundamental perspective of understanding the role of size and confinement on their physics and by the extreme technological relevance of their properties. Among the wide variety of magnetic nanoparticles susceptible to be modified in order to manipulate their properties, spinel ferrite nanoparticles are of the most attractive systems. The reason is that, compared to the crystal structure of other magnetic nanoparticles (elemental, intermetallic, oxides), the spinel structure is complex and adaptive, and thus it can be modified in various ways, resulting in novel or enhanced physical properties. Therefore, spinel ferrites nanoparticles consist one of the most versatile experimental environments to probe the fundamental and applied behavior of magnetic nanoparticles. The spinel structure, which will be described below, is characterized by three degrees of freedom associated with the detailed atomic arrangement: (i) the lattice parameter, $a$; (ii) the anion parameter, $u$; and (iii) the cation inversion parameter, $i$. For spinel nanoparticles, these degrees of freedom can be modified controllably by changes of the preparation method and/or the particle-size, by doping and by processing.

The present study has been undertaken against the above background. It is focused on the effect of doping on the above-mentioned degrees of freedom of the spinel structure and concomitantly on the magnetic properties of the $Zn_{1-x}In_xFe_2O_4$ nanoparticles with $0 \leq x \leq 0.6$. This study is part of a comprehensive investigation on the effects of preparation conditions, particle size, various dopants and processing on the structure and the physical properties of spinel ferrite nanoparticles. The ultimate purpose is to establish the structure–property–function relationship and identify promising materials for applications.

The entire solid solution $Zn_{1-x}In_xFe_2O_4$ ($0 \leq x \leq 0.6$) adopts the spinel structure. Sickafus et al.[1] examines the spinel structure

* Corresponding author at: National Center for Scientific Research "Demokritos", Institute of Materials Science, Corner Neapoleos and Patriarchou Grigoriou Streets, 15310 Agia Paraskevi (Athens), Greece. Tel.: +30 210 6503320; fax: +30 210 6519430.
*E-mail address:* evagelia@ims.demokritos.gr (E.G. Moshopoulou).

0955-2219/$ – see front matter © 2007 Elsevier Ltd. All rights reserved.
doi:10.1016/j.jeurceramsoc.2007.02.165

in detail. The majority of spinel compounds belong to the space group *Fd*3*m*. The conventional spinel cell $AB_2O_4$ is a cubic face centered unit cell containing $Z = 8$ formula units. There are 96 interstices between the anions in the spinel cell; however, in $AB_2O_4$ compounds, only 24 are occupied by cations. Of the 64 tetrahedral interstices that exist between the anions, 8 are occupied by cations. The remaining 16 cations occupy half of the 32 octahedral interstices. Many compounds that adopt the spinel structure can accommodate significant amounts of disorder. In the "normal" spinel, the cations A occupy the tetrahedral sites and the cations B occupy the octahedral ones. In the "inverse" spinel half of the B cations occupy the tetrahedral sites while A cations and the other half of the B cations occupy the octahedral sites. The variable $i$ is the so-called inversion parameter, which specifies the fraction of tetrahedral sites occupied by the B cations. For a normal spinel, $i = 0$, for random arrangement, $i = 2/3$, and for an inverse spinel, $i = 1$. The cations A and B are at the special positions (1/8, 1/8, 1/8) and (1/2, 1/2, 1/2) of the space group *Fd*3*m* (origin $\bar{3}m$), respectively. The anions are at the general position ($u$, $u$, $u$); therefore, the only variable atomic coordinate of the spinel structure is the parameter $u$.

## 2. Experimental

Nanoparticles of composition $Zn_{1-x}In_xFe_2O_4$ ($x = 0$, 0.15, 0.3, 0.45 and 0.6) were prepared by a low-temperature chemical co-precipitation method[2] using aqueous solutions of nitrate precursors. Stoichiometric amounts of $Fe(NO_3)_3{\cdot}9H_2O$ (Merck, Germany) and $Zn(NO_3)_2{\cdot}6H_2O$ (Merck) were dissolved in distilled water and mixed with appropriate amount of aqueous $InCl_3$ solution (obtained by mixing $In_2O_3$ (Merck) with HCl). Sodium hydroxide was used as a precipitating alkali. The co-precipitation reaction was carried out at 80 °C for 60 min under continuous stirring. The precipitates were separated from the slurry by centrifuging and washed a number of times with distilled water and then with absolute ethanol. The nanoparticles formed were dried at 120 °C for 1 day and finally dry milled in a mortar.

Conventional powder X-ray diffraction was initially carried out in order to identify all the phases present and determine the particle size. The experiments were carried out on a Siemens D500 diffractometer with a step size 0.03°/15 s, using filtered Cu Kα radiation with wavelength 1.506 Å. Transmission electron microscopy (TEM), high resolution transmission electron microscopy (HRTEM) and energy dispersive X-ray spectroscopy (EDXS) experiments were performed in order to probe the microstructure of the nanoparticles $Zn_{1-x}In_xFe_2O_4$, determine their composition and confirm their particle size obtained previously by X-rays. Specimens of $Zn_{1-x}In_xFe_2O_4$ were prepared for TEM by dissolving the nanocrystal powder in high purity ethanol. A drop of the resulting suspension was deposited onto a lacey carbon film supported on a copper grid. The $^{57}$Fe Mössbauer spectra were recorded at −268.95 °C on a conventional constant acceleration spectrometer with a $^{57}$Co(Rh) source moving at room temperature (RT). Isomer shift values are quoted with respect to metallic iron at RT. Micro-Raman measurements were carried out at RT, using a Jobin-Yvon triple spectrometer T64000 equipped with a charge-coupled device for detection of the signal. Excitation was carried out with the 532.1 nm line of a doubled Nd:YAG crystal laser with a power of 0.1 mW focused to a spot of 1 μm on the sample.

## 3. Results and discussion

### 3.1. Powder X-ray diffraction

Fig. 1 shows the X-ray diffraction patterns of the nanoparticles $Zn_{1-x}In_xFe_2O_4$. The spinel phase is present in all samples and has been unambiguously indexed. These data showed that the samples $Zn_{1-x}In_xFe_2O_4$ with $x \leq 0.3$ are single phase. However, TEM data (discussed below) revealed that only the $ZnFe_2O_4$ and $Zn_{0.85}In_{0.15}Fe_2O_4$ samples are indeed single spinel phase. The rest of the samples are composed of the spinel phase and a second phase which is $In(OH)_3$. This second phase is present in very small quantities in the samples $Zn_{1-x}In_xFe_2O_4$ with $x = 0.2$, 0.25, 0.3 and it could not be detected by X-rays. The average size of the nanoparticles estimated by the Sherrer equation, $d = 0.9\lambda/\beta(\cos\theta)$, are 4.1, 3.0, 2.4, 2.3 and 2 nm for $x = 0$, 0.15, 0.20, 0.25 and 0.3, respectively. The particle size decreases as a function of $x$, suggesting that in In-rich nanoparticles the surface effects are quite pronounced. The cell constant $a$ increases as a function of $x$ implying that indium indeed enters into the structure.

### 3.2. Transmission electron diffraction and energy dispersive X-ray spectroscopy

HRTEM and the corresponding selected area diffraction (SAD) pattern of $ZnFe_2O_4$ nanoparticles are illustrated in Fig. 2a. The nanoparticles exhibit sizes of about 4–6 nm, which is in very good agreement with the value obtained from the X-ray diffraction data. Each nanoparticle is single crystalline and, consequently, the SAD pattern (Fig. 2a, inset) obtained from a wide area is comprised of diffraction rings with several Bragg spots revealed. The d-spacings deduced from the diffraction pat-

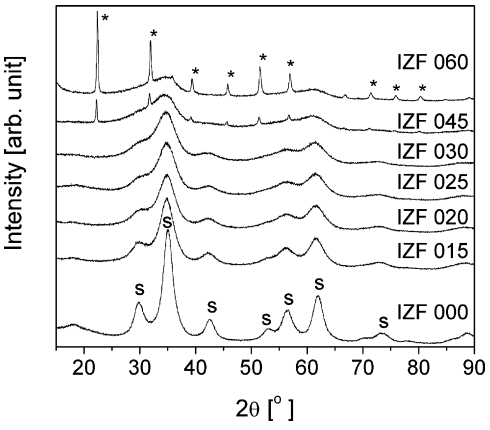


Fig. 1. XRD patterns of the $Zn_{1-x}In_xFe_2O_4$ nanoparticles, *s* represents the spinel phase, asterisk represents the $In(OH)_3$ (in the sample notation, letters and numbers indicate the system and indium concentration used, e.g., IZF 015 corresponds to the sample $Zn_{0.85}In_{0.15}Fe_2O_4$).

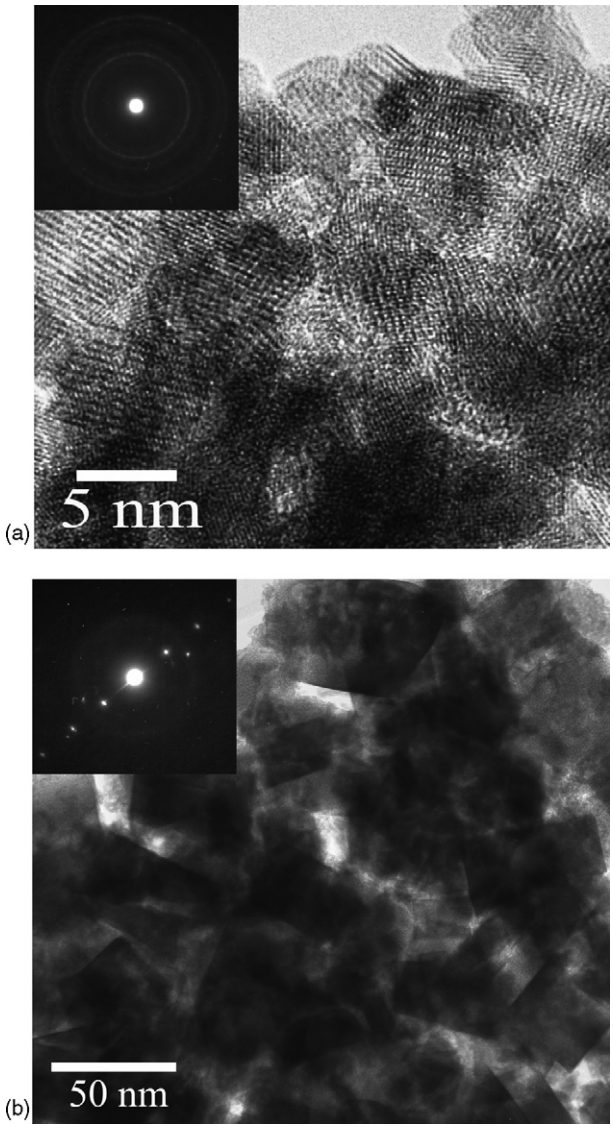


Fig. 2. TEM images of the $ZnFe_2O_4$ (a) and $Zn_{0.4}In_{0.6}Fe_2O_4$ (b) samples.

terns correspond to the spinel structure. The composition of the nanoparticles, obtained by EDXS analysis, corresponds to the expected chemical formula $ZnFe_2O_4$ (within the accuracy of the EDXS analysis).

The TEM image of the sample with nominal composition $Zn_{0.4}In_{0.6}Fe_2O_4$, Fig. 2b, reveals that the sample consists predominantly of a highly crystalline phase and the spinel nanoparticles are the minority phase. The series of single crystal spots in the SAD pattern insert in Fig. 2b which are superimposed in the diffuse rings of the ferrite structure in the pattern corresponds to $In(OH)_3$. EDXS analysis suggests that the Zn/In ratio in the phase is more than 1/4 within the experimental error of the EDXS measurement.

The nanoparticles with compositions between $ZnFe_2O_4$ and $Zn_{0.4}In_{0.6}Fe_2O_4$ exhibit structural characteristics intermediate between the features of these two end-members. The particle size decreases slightly as the In-content $x$ increases (again in agreement with the conclusions drawn from the X-ray data) and the quantity of the second phase increases as $x$ increases as well.

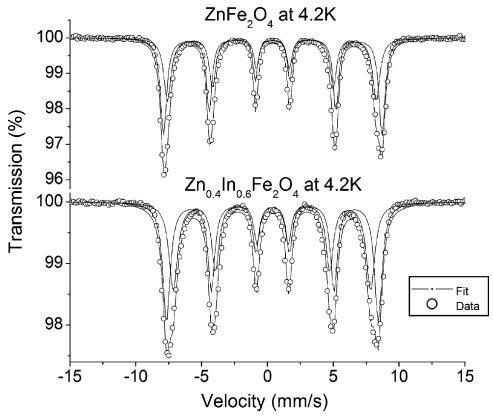


Fig. 3. Mössbauer spectra of the $ZnFe_2O_4$ and $Zn_{0.4}In_{0.6}Fe_2O_4$ samples at −268.95 °C (4.2 K).

### 3.3. Mössbauer spectroscopy

Mössbauer spectra were taken at −268.95 °C for the two end-members $ZnFe_2O_4$ and $Zn_{0.4}In_{0.6}Fe_2O_4$. The two spectra are similar with slightly broader lines and lower hyperfine fields observed in the In-substituted sample (Fig. 3). Both spectra require two subspectra for a satisfactory fit of the data. The need of two subspectra has been attributed to areas of short and long-range order, which also lead to broadening of the magnetic transition.[3] A degree of inversion in nanoparticle samples has also been suggested[4] as the source of the two subspectra. In order to distinguish between these two options, spectra obtained in an applied magnetic field are required. In either case, it is clear that there is a degree of disorder in the occupancies of A and B sites by the cations.

### 3.4. Raman spectroscopy

Raman scattering measurements were carried out for the $ZnFe_2O_4$ and $Zn_{0.4}In_{0.6}Fe_2O_4$ samples. The spectra (Fig. 4) of the samples in the 200–800 $cm^{-1}$ range are fitted with four broad lines (FWHM about 60–100 $cm^{-1}$) at 350, 505, 647 and 693 $cm^{-1}$. For $ZnFe_2O_4$, which approaches the normal spinel structure, the high frequency mode at 693 $cm^{-1}$ is less pronounced.[5] The $AB_2O_4$ spinel structure permits five active Raman modes ($A_{1g} + E_g + 3T_{2g}$). It is generally accepted that the

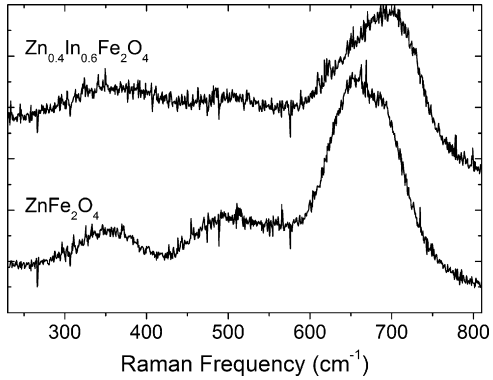


Fig. 4. Raman spectra of $ZnFe_2O_4$ and $Zn_{0.4}In_{0.6}Fe_2O_4$ samples at RT.

modes above 600 $cm^{-1}$ are of the $A_{1g}$ type, involving motions of the O in tetrahedral $AO_4$ groups.[5] Therefore, the observation of two modes above 600 $cm^{-1}$ can be due to coexistence of two $AO_4$ groups, A being either Zn or Fe. In fact, the 647 $cm^{-1}$ is attributed to the oxygen breathing vibrations against zinc, in accordance to ref.[5] while the high frequency one at 693 $cm^{-1}$ is due to the corresponding oxygen vibrations against iron.

Fig. 4 shows that the introduction of In induces significant positive frequency shifts of about 15 $cm^{-1}$ for both $A_{1g}$ modes, showing off that In is incorporated into the structure. The frequency shifts observed are reasonably due to the strong coupling of the oxygen atoms with In, considering that the last has much larger ionic radius than the other cations.

## 4. Conclusions

$Zn_{1-x}In_xFe_2O_4$ ($0 \leq x \leq 0.6$) nanoparticles were prepared by using a co-precipitation method. The spinel structure is maintained for the whole solid solution. While indium enters into the spinel structure for all $x$ investigated, only $Zn_{0.85}In_{0.15}Fe_2O_4$ can be formed as single phase. For $x \geq 0.20$, a second phase, $In(OH)_3$, is formed. The average particle size decreases as $x$ increases. Mössbauer and Raman spectroscopy revealed that site disorder is present between Zn, Fe and In in the spinel cell.

## References

1. Sickafus, K. E., Wills, J. M. and Grimes, N. W., Structure of spinel. *J. Am. Ceram. Soc.*, 1999, **82**(12), 3279–3292.
2. Maletin, M., Cvejić, Ž., Rakić, S., Nikolić, Lj. M. and Srdić, V. V., Low-temperature synthesis of nanocrystalline $ZnFe_2O_4$ powders. *Mater. Sci. Forum*, 2006, **518**, 91–94.
3. Schiessl, W., Potzel, W., Karzel, H., Steiner, M., Kalvius, G. M. *et al.*, Magnetic properties of the $ZnFe_2O_4$ spinel. *Phys. Rev. B*, 1996, **53**, 9143–9152.
4. Choi, E. J., Ahn, Y. and Song, K.-C., Mössbauer studies in zinc ferrite nanoparticles. *J. Magn. Magn. Mater.*, 2006, **301**, 171–174.
5. Wang, Z., Schiferl, D., Zhao, Y. and O'Neill, H. St. C., High pressure Raman spectroscopy of spinel-type ferrite $ZnFe_2O_4$. *J. Phys. Chem. Solids*, 2003, **64**, 2517–2523.